The influence of spatial properties of sessile benthic organisms, transect re-location and sampling effort on monitoring outcomes for visual surveys

Nicholas R. Perkins[1]

Geoffrey R. Hosack[2]

Scott D. Foster[2]

Nicole A. Hill[1]

Neville S. Barrett[1]

[1] **Institute of Marine and Antarctic Studies, University of Tasmania**

[2] **Commonwealth Industrial and Scientific Research Organisation, Australia**

Corresponding author:

Nicholas.Perkins@utas.edu.au

Abstract

1. Monitoring the impacts of pressures, such as climate change, on marine benthic ecosystems are of high conservation priority. Novel imaging technologies such as autonomous underwater vehicles (AUVs), remotely operated vehicles (ROVs) and towed systems now give researchers the ability to monitor benthic ecosystems over large spatial and temporal scales.
2. The design of monitoring programmes that utilize such technologies is currently hindered by a lack of information about the typical abundance and spatial distributions of target indicators and the level of sampling required to detect changes. A further complicating factor is that these sampling platforms are often not able to be exactly relocated when conducting repeat surveys.
3. How the spatial properties of benthic organisms influence estimates of cover given alternative designs that vary in the geolocation precision of transects and the sampling intensity of images is explored. A geostatistical modelling approach is used to quantify the spatial distribution of 20 key deep-water invertebrate species at a long-term monitoring site. The parameter estimates from these models are then used to simulate repeat transects with geolocation error and different levels of sampling.
4. Results suggest that species with short effective ranges (i.e., those with strong spatial dependence over relatively short distances) and large spatial variance, which suggests strong spatial dependence effects, will require greater sampling effort to achieve a given standard of precision.
5. Spatial offsets of 2 metres, typical of an AUV, are unlikely to have dramatic impacts on the precision of estimates when sufficient images are sampled, but offsets of 10

metres that are typical of towed systems may require prohibitively high sampling effort for some species. These findings have important implications for benthic monitoring programmes and highlight the importance of considering the interaction between sampling design, the technical limitations of survey equipment and the spatial properties of indicator species.

Keywords: AUV, benthic monitoring, geostatistical modelling, sampling design, species distributions

1. Introduction

In marine ecosystems, benthic habitats play a key role, support important fisheries, and contain rare or threatened species (Hughes, Bellwood, Folke, Steneck, & Wilson, 2005). Furthermore, benthic ecosystems are under increasing pressure, in particular from anthropogenic sources such as climate change and fishing (Halpern et al., 2008). Monitoring changes to these ecosystems is therefore an essential step toward understanding the impacts of such pressures and informing management and policy decisions that aim to mitigate adverse impacts. Although monitoring and process-based understanding of dynamics in shallow waters is reasonably well established via scuba-based surveys and manipulative studies (e.g. Babcock et al., 2010; Molloy et al., 2013), the quantitative assessment of benthic ecosystems at greater depths (i.e. >30 m) is still in its infancy (Boavida, Assis, Reed, Serrão, & Gonçalves, 2015; Schlacher, Williams, Althaus, & Schlacher-Hoenlinger, 2010). Advances in digital imaging technologies are now beginning to address this knowledge gap. This imagery is typically acquired from platforms such as autonomous underwater vehicles (AUVs), remotely operated vehicles (ROVs), and imaging sleds that collect large volumes of high quality benthic imagery over broad scales (Beijbom et al., 2015; Williams et al., 2012). This imagery, and the ability to make repeated observations over time, now enables researchers to monitor temporal changes in deep-water benthic habitats and their associated biological populations.

When the aim is to detect chronic impacts such as the effect of long-term fishing and climate change that occur over broad spatial scales, monitoring programme designs must involve multiple sites that span large geographical domains (Brown et al., 2011; Parmesan, Duarte, Poloczanska, Richardson, & Singer, 2011). Technologies such as AUVs and ROVs are capable of operating over these scales, and programmes utilizing these platforms with transect based methods at multiple sites across regions have now been established (e.g. http://imos.org.au/auv.html, Whiteman et al. (2013) and Karpov et al. (2012)). Monitoring with sufficient statistical precision to effectively describe indicator abundance for any given site, and how it changes through time, for programmes operating over large scales is not a trivial task. The inherent spatial and temporal variability in biological systems, and the ability of the design of these programmes to meet monitoring objectives needs to be thoroughly assessed.

Imagery-based surveys have hierarchical (nested) spatial scales: regional, sites, transects and images. For large-scale monitoring programmes, interest is typically directed at detecting change at a site, or across a network of sites within a region through time, and thus precise estimates at a site level are important for achieving high statistical power (Elston, Nevison, Scott, Sier, & Morecroft, 2011; Larsen, Kincaid, Jacobs, & Urquhart, 2001). At a site level, transect-based surveys must account for the interaction between sampling effort, the spatial accuracy of repeat surveys and the distributional properties of species (e.g. Molloy et al., 2013; Perkins, Foster, Hill, & Barrett, 2016; Ryan & Heyward, 2003). Sampling design choices for benthic image-based deployments, and for all taxonomic units, include transect layout (Foster et al., 2014), the method and number of images selected, and the number of points used to score individual images (Brown et al., 2004; Leujak & Ormond, 2007). Ideally, sampling design should take the properties of indicators into account (Legendre et al., 2002); however, in comparison to shallow water systems, there is a lack of detailed information regarding the distribution, abundance and patchiness of benthic organisms. For continental shelf ecosystems beyond scuba diving depths, researchers are finding that diversity is often high and there is a lack of dominant space occupiers, and hence many potential indicators are likely to have low cover due to their relatively small size and/or sparse distribution (Monk et al., 2016; Schlacher et al., 2007; Williams, Althaus, & Schlacher, 2015). In addition, the technical difficulties associated with surveying deep-water benthic habitats means that it may not always be possible for repeat transects that cover these reef systems to exactly sample the same image locations on every successive deployment. The final choice of a particular indicator relies on many factors that relate to the specific objectives of particular monitoring programmes. However, such choices must also take into account the combination of potential low overall cover, the spatial attributes of a species' distribution, and transect geolocation precision. These latter factors may have important consequences for the ability of monitoring programmes to detect change in a particular choice of indicator.

Previous research has shown that for short (10 – 50 m) straight-line benthic transects, the accurate retracing of marked transects can dramatically increase the precision of estimates and the ability to detect change (Brown et al., 2004; Ryan & Heyward, 2003; van der Meer, 1997); however, surveys by platforms such as AUVs, ROVs or imaging sleds are often conducted over larger scales, often with survey designs that are not simple straight-line transects, and in these situations marking transects is problematic (Pizarro et al., 2013; Van Rein, Brown, Quinn, & Breen, 2009). For example, Huvenne et al. (2016) note the difficulty in navigating precise repeat transect lines with these technologies in deep water. AUVs with their on-board sensors may offer some advantages for repeat surveys, with pre-programmed flight paths that are conducted with mean repeat geolocation precision of 1-2 m (unpublished data), whereas other potential survey platforms are likely to have repeat geolocation precision of tens of metres, dependent on water depth (Williams et al., 2015). The distance at which an offset transect will degrade survey outcomes is currently unclear, and this threshold distance will be inextricably linked to the spatial properties of the chosen indicator organisms.

The influence of the spatial properties of organisms and the effect of spatial autocorrelation on survey outcomes is being increasingly recognized (Andrew & Mapstone, 1987; Legendre, 1993; Tobin, 2004). Auto-correlated data that arises from spatial dependence are likely commonplace when sampling biological systems, and failure to account for this autocorrelation can lead to erroneous statistical conclusions and deflated estimates of uncertainty (Horne & Schneider, 1995). Conversely, prior knowledge of the spatial properties of indicators, when available, can be used to improve sampling designs and survey outcomes (Legendre et al., 2002). Here, a geostatistical modelling approach (e.g. Diggle & Ribeiro, 2007) is used to quantify spatial patterns in species distributions at a deep-water monitoring site. The models explicitly account for spatial autocorrelation, and the statistical descriptions of spatial distributions they provide allow the comparison of spatial properties across different organisms and systems. In this context, two important parameters are particularly useful in the statistical description of spatial patterns: the spatial variance and the range. The range describes how spatial dependence (or spatial correlation) decays with distance and is often quantified as the “practical” or “effective” range, which is the distance at which the correlation between observations is less than 0.1 (Lindgren, Rue, & Lindstrom, 2011); the spatial variance determines the magnitude of variability at a given distance (Banerjee, Carlin, & Gelfand, 2004). The parameter estimates for the intercept (i.e., mean cover), spatial range and variance from the models are used to evaluate how offset repeat transects and different levels of sampling effort impact both the precision of estimates of cover for monitoring targets and the ability to detect changes in cover through time.

This study investigates: (1) the spatial properties of typical deep-reef sessile invertebrates, (2) how these influence the geolocation precision required for repeat surveys, and (3) the level of image sampling necessary to achieve effective benthic monitoring programmes for typical species of interest. The distributional properties of 20 deep-water sessile species (potential indicators) are investigated across a long-term survey site. Geostatistical models, which are conditioned on the observed imagery data, are used to predict how the spatial properties of these species affect the precision of cover estimates and the ability to detect change. This is achieved by simulating repeat transects with varying geolocation inaccuracies and differing image sampling scenarios across the modelled spatial surface. The simulations incorporate the breadth of likely distributional parameters for each species. In this way, results are provided that incorporate a wide range of potential distributions, and develop recommendations that are likely to be valid across a wide variety of benthic ecosystems.

2. Materials and methods

2.1 Data collection

The study site chosen for analyses is a deep-water reef located off the east coast of Tasmania, Australia within the Freycinet Australian Marine Park (Figure 1) and is part of a long-term monitoring programme within the Integrated Marine Observing System (IMOS) programme (see http://imos.org.au/). The goals of this program include examining the impacts of large-scale processes across a network of sites. Assessing the survey precision necessary to detect change at an individual site that can be detected is an important first step. To test this ability, a transect conducted on the 13th June, 2014 is used as the basis for analysis. A transect is defined here as the continuous path navigated by the AUV (Figure. 1). The transect surveyed benthic sessile invertebrate fauna associated with a granite reef outcrop at 60-85 m depth. The total length covered by the transect was approximately 3500 m. The AUV's on-board sensors maintained a relatively constant altitude of approximately 2 m above the reef during the survey resulting in an image footprint of approximately 1.6 x 1.3 m (~ 2 m^2), allowing consistent identification of distinctive biota within the acquired imagery.

A subset of 20 'morphospecies' (see Supplementary Materials for example photos and a brief description of each) were selected as model potential indicator species for this reef system. The three selection criteria were as follows: (i) the morphospecies were distinctive and easily identifiable within imagery, (ii) the morphospecies had a wide latitudinal gradient of distribution known from prior image-based analyses conducted elsewhere on the east coast of Australia, and hence were potentially useful indicators at greater spatial scales, and (iii) initial investigation showed these morphospecies to be the most abundant at the study site. This last criterion is important because most of the morphospecies across the region have relatively low cover (unpublished data), and only the more abundant species are likely to be suitable as indicators due to the sampling effort required to quantify rare species over time (Skalski, 2012). Morphospecies here refers to groups identified from imagery that have characteristically different morphologies and/or colours than others within the same taxonomic grouping. They are assumed to represent species, but were not officially taxonomically identified as no physical samples were taken. This approach is commonly taken in studies that utilize benthic imagery (e.g. James, Marzloff, Barrett, Friedman, & Johnson, 2017 ; Schlacher et al., 2010; Williams, Althaus, Barker, Kloser, & Keith, 2007) and has proven useful for characterizing benthic communities and detecting change (Brind'Amour et al., 2014). Hereafter these morphospecies will be referred to as “species”. The 20 species chosen were all sessile invertebrate fauna which are typically found in depths greater than 30 metres, below the zone dominated by macroalgae across the region studied (Shepherd & Edgar, 2013).

Detailed scoring of the AUV imagery was conducted to quantify the percentage cover and distribution of the 20 species. All images that were completely sand were excluded from the analysis because all of the selected species are reef-associated species. Due to the velocity of the AUV and the frame rate of the imagery collected, adjacent images typically overlap. Therefore, every fifth image (giving 622 images) along the transect was selected to give essentially continuous, but not overlapping, image coverage. Transect Measure software (http://www.seagis.com.au/transect.html) was then used to score the selected images. Fifty random points were placed on each image and the number that fell on any one of the 20 species was recorded. Fifty points typically gives relatively high precision in cover estimates for an image (Perkins et al., 2016) and this is the number of points commonly used for scoring AUV imagery within the IMOS AUV program.

2.2 Geostatistical modelling

A model-based geostatistical analysis was used to examine the spatial properties of each species (e.g. Diggle & Ribeiro, 2007). The model used was a spatial Bayesian binomial regression model with a logit link function:

$$(1) \quad y(s_i, c) \sim Binomial(n, p(s_i, c))$$

$$(2) \quad log\left(\frac{p(s_i,c)}{1 - p(s_i,c)}\right) = \alpha_c + z(s_i, c)$$

$$(3) \quad z(s_i, c) \sim N(0, \Sigma(\rho_c, \sigma_c^2))$$

$$(4) \quad \alpha_c \sim N(0, b_\alpha^2)$$

$$(5) \quad log\rho_c \sim N(a_\rho, b_\rho^2)$$

$$(6) \quad log\sigma_c \sim N(a_\sigma, b_\sigma^2)$$

where $y(s_i, c)$ is the number of points in an image at location s_i where species c is observed out of a total of $n = 50$ points, $p(s_i, c)$ is the estimated percentage cover of species c at location s_i with *i* indexing the image location, α_c is the intercept for species c, and $z(s_i, c)$ is the latent spatial random field whose autocorrelation is governed by a Matérn covariance function (see details in Appendix) with autocorrelation parameter ρ_c, and spatial variance σ_c^2. Equations (5) and (6) complete the Bayesian model and values with hyperparameters a_ρ, b_ρ^2 and a_σ, b_σ^2 are given in the Appendix. Informally, the hyperparameters are chosen so that the effective spatial range is in the order of tens of metres. The inclusion of the spatial dependence terms allow for the existence of missing covariates by directly addressing spatial autocorrelation (Banerjee et al., 2004; Barry & Elith, 2006; Legendre, 1993). The model reflects the current state of knowledge that could be used in designing a monitoring plan.

Estimation of model parameters and prediction was conducted by using the Integrated Nested Laplace Approximation (INLA) method (Rue, Martino, & Chopin, 2009). The INLA approach to estimation of a Bayesian model utilizes an analytical approximation to the parameters' posterior distribution. The spatial model is represented in INLA by using a discrete spatial random process approximation for the (continuous) latent spatial random field z (i.e. a Gaussian Markov random field; Blangiardo & Cameletti, 2015; Lindgren et al., 2011).

For each of the 20 species, 5000 sample draws of the parameters were taken from the INLA analytical approximation to the posterior distribution. These posterior samples were used to quantify the characteristics of the species in the simulation study described below.

2.3 Simulation of repeat transects and image sampling intensities

To examine the effectiveness of attempting to conduct repeat surveys for the 20 species, the posterior samples of the parameters were used to simulate spatial surfaces on to which random repeat transects were overlaid. The differences in the mean estimate of the cover of each species were calculated for simulated repeat transects located at varying offsets from the original transect location, and various image sampling intensities. The offset distances between the original and simulated transects were: 0.5, 1, 2, 4, 8, 16, 32, 64, 128 metres. This represents a wide range of spatial offsets that span the range of re-deployment precisions that are expected for benthic survey platforms, extending from AUVs (most accurate method) to towed video (least accurate method). The effect of including a different number of sampled images by varying a systematic sample along the transect was explored. Image sampling intensities tested were every 5th (622 images), 20th (156 images), 50th (62 images), 100th (31 images) and 200th image (16 images). These sampling intensities correspond to sampling approximately every 2, 10, 20, 40 and 80 m along the transect.

The simulation approach consisted of the following steps for each of the 5000 posterior samples of parameters available for each species:

Step 1. Generate a set of image locations that represented a repeated transect, with: (i) a specified offset distance and random angle of deflection from the original transect image locations, and (ii) a specified systematic image sampling intensity with a random starting point along the transect.

Step 2. Generate a stationary Gaussian random field (GRF) at all image locations using a random multivariate normal distribution with mean zero and a covariance matrix created using the sampled parameter values and distances generated in step 1.

Step 3. GRF values were added to the sampled intercept parameter value to determine the log-odds of presence at any given image location (see equation 2 above). This value was then inverse-logit transformed and used to calculate the probability $p(s_i, c)$, of a point landing on a particular species within the given image. A binomial random variable was then generated for $y(s_i, c)$. That is, $y(s_i, c)$ is the number of points out of 50 that fell on a particular species within a given image, see equation (1).

Step 4. The percentage cover estimate for both the original transect and repeat transect were then calculated as the mean of the image percentage covers, where the image percentage cover was estimated by the number of ‘hits’ divided by 50. The difference between these cover estimates was stored for each simulation.

Steps 1-4 were completed for each of the 5000 joint parameter posterior draws for each of the 20 species. The precision of repeat transects was quantified by examining the variability across simulation runs between a transect with full image sampling in the original position compared to spatially offset transects with different levels of image sampling. Formally, this was calculated as the difference in the coefficient of variation (delta CV; the standard error divided by the mean) of the percentage cover estimates from a transect in the original position with all images sampled (every 5thimage) compared to the offset transects with varying image sampling intensities over the simulation runs. A smaller delta CV indicates more precise estimates in cover between the two sampling occasions. Change in CV was chosen as the metric to quantify precision, as it allows a unitless measure of precision that accounts for differing mean covers.

2.4 Change detection simulations

To examine if transects with different offsets and image sampling schemes were able to detect temporal change, a halving in the odds of presence was simulated for each species. A halving in the odds of presence was chosen as an example scenario as many of the species are expected to decline in cover across this region with ongoing climate change (see Perkins, Foster, Hill, Marzloff, & Barrett, 2017). A change in the odds of presence was the natural choice as the model was binomial with a logit link function. Two offsets (2 metres and 10 metres, indicative of typical AUV redeployment accuracy and a best-case scenario for towed video respectively) and four image sampling intensities (every 5th, 20th, 50th and 100th image) were explored. Image sampling represents a range of image sampling from every nonoverlapping image (every 5th) to the level of sampling that has been previously employed in scoring AUV imagery within the IMOS programme (every 100th).

Again the INLA approach was used. Steps 1 and 2 from above were repeated with the same model parameters and priors as outlined above. At step 3, a halving in the odds of presence was induced for the repeat transect. A halving of the odds of presence approximately corresponds to a 50% decrease in the probability of presence of a species within any given image when percentage covers are less than 5% (i.e. for all the species considered in this study). A new INLA model was fitted to the combined data set of original and offset transect data, including a binary factor coded 0 for the original transect and 1 for the repeat transect, termed here as the ‘temporal effect’. This time 1000 posterior sample draws were used, and the posterior distribution of the temporal effect was recorded for each set of posterior samples. One thousand samples were used for this portion of the study due to the computational load involved in estimating a large number of models. For each sample drawn from the posterior, the probability that the temporal effect was less than zero was estimated. These estimated probabilities of a negative temporal effect were averaged over the 1000 posterior sample draws. The resulting mean is reported as the probability of detection of temporal decline.

3. Results

3.1 Data summary and model parameter estimates

Percentage covers for the 20 species were very low, despite a number of them being present in a relatively high proportion of the imagery (Table 1). The majority of species had distributions that exhibited high levels of spatial dependence, with short effective ranges (Table 1, Figure 2), indicating spatial autocorrelation over small spatial scales. Of the 20 species modelled, 11 had mean effective ranges of less than 5 metres, and only six had mean effective ranges greater than 20 metres. The posterior distributions of the range for all 20 species are shown in Figure 2.

The estimates of spatial variance for each species encompassed a wide variety of values (Table 1), and when considered in combination with the effective range for an individual species, provided a useful quantitative description of the spatial distribution of species across the site. Species that occurred in a relatively large proportion of images (i.e. > 20% of images, e.g. Gorgonian sp., Erect sponge sp. 3, Massive sponge sp. 1 – see Table 1) tended to have lower spatial variance than those that had lower cover (e.g. Black coral sp. and Cup sponge sp. 5 – see Table 1), particularly when those species with low overall cover had a few images with higher cover (e.g. Black coral sp. – see also Figure 3 a). Species with shorter effective ranges, and lower spatial variance tended to occur in smaller clusters that were relatively evenly distributed over the transect (e.g. Erect sponge sp. 3 – see Figure 3 a).

3.2 Simulation of offset transects

Results are presented for six species that are representative of the spectrum of effective ranges, spatial variances and cover of all 20 species. Results for the remaining species can be found in the Supplementary Materials. The distributions of these six species across the original transects based on the empirical data are shown in Figure 3a. The estimated posterior mean and 95% credible intervals of the mean differences in the estimated percentage cover are shown in Figure 3b. This bias (i.e. mean difference) for the estimated percentage cover between the original and offset transects was smallest at small offsets (<4 m). The posterior estimate of the mean difference tended to be small and no consistent pattern of over or under estimation of percentage cover was observed for any species. In contrast, credible intervals of the mean difference expanded more rapidly with offset distance for species with short ranges (e.g. Erect sponge sp. 3, Black coral sp. and Erect sponge sp. 1 – Figure 3b), and more slowly for species with longer ranges (e.g. Gorgonian sp. and Laminar sponge sp. 2 – Figure 3b). The increasing width of the credible intervals demonstrates greater uncertainty in the mean difference with increasing offset distances.

The precision of estimates between repeat transects was associated with the spatial variance of each species (Figure 4 and Table 1). Ideally, the difference in CV (i.e. delta CV) between repeat transects should be zero (i.e. a high precision), and hence the greater the delta CV the less precise are the estimates of cover. Cover estimates for offset transects were less precise for species with larger spatial variances (e.g. Black coral sp., Cup sponge sp. 5, Erect sponge sp. 1 - Table 1).

All species showed a consistent pattern of increased delta CVs between transect estimates with increased offset distances, with the major differences being the distance at which delta CVs approached an asymptote (Figures 4 and 5). The estimated delta CV reached an asymptote at longer offset distances for species with longer range parameters (e.g. Gorgonian sp. and Cup sponge sp. 5) compared to those with shorter range parameters. Species with short range parameters (e.g. Black coral sp., Erect sponge sp. 1 and Erect sponge sp. 3) generally reached the asymptote within a 10 metre offset distance. The exception to this pattern was Laminar sponge sp. 2 which showed an erratic relationship with offset distance. This species was rare within the sample, with very low coverage (see Table 1).

3.3 Simulation of offset transects with different image sampling intensities

The delta CV of cover estimates unsurprisingly decreased with sampling intensity; however, the rate at which delta CV decreased (see Figure 5 and S1 Supplementary Materials) was particularly dependent on the effective range, and to a lesser extent the spatial variance of each species. This effect was most pronounced for the species with shorter ranges (Black coral sp., Erect sponge sp. 1, Erect sponge sp. 3), which all showed a greater decreases in delta CVs with increased image sampling than those with longer ranges (e.g. Gorgonian sp. and Cup sponge sp. 5).

3.4 Probability of detecting a decrease in the cover of target species

The difference between a 2 and 10 metre offset in repeat transects had a large effect on the probability of detecting the ~50 % simulated decrease in the cover for species with high spatial variance and short ranges (e.g. Black coral sp., Erect sponge sp. 1, Cup sponge sp. 1, Cup sponge sp. 2; Table 1, Figure 6 and S2 Supplementary Materials) at equivalent levels of sampling.

The image sampling intensity was an important factor determining the probability to detect the simulated change, with sampling every 5th image providing >80% probability of detecting change for 17 out of the 20 species regardless of the offset distance. The three species for which 80% probability of detection (of temporal decline) could not be achieved were the three species with the lowest abundance (Laminar sponge sp. 2 – Figure 6; Massive sponge sp. 4 and Laminar sponge sp. 3 S2 Supplementary Materials).

The effect of the geolocation error became more apparent with decreased image sampling intensity. For example, sampling every 20th image provided >80% detection probability of temporal decline for 17 out of 20 species with a 2 m offset, but only 13 out of 20 species with a 10 m offset. Sampling every 50th image with a 2 m offset provided >80% detection probability for 16 species, whereas sampling every 50th image with a 10 m offset only provided >80% probability of detecting the temporal decline for only 10 species.

Species whose change in cover could be detected with high probability with a 2 m offset, but not a 10 m offset with the same image sampling intensity were consistently those species with relatively high spatial variance and short ranges (e.g. Black coral sp., Cup sponge sp. 1, Cup sponge sp. 2 and Cup sponge sp. 4 when sampling every 50th image – Figure 6 and S2 Supplementary Materials).

4. Discussion

Understanding the effect of spatial and temporal patterns is a necessary prerequisite for the design of effective monitoring programmes that aim to detect spatial and temporal change (Urquhart, Overton, & Birkes, 1993). In deep-water benthic ecosystems, where researchers often find high diversity and low overall cover of single species (e.g. Monk et al., 2016; Schlacher et al., 2007) and the spatial precision of transects is problematic, it is particularly important that sampling designs take into account the spatial properties of organisms (Irvine et al., 2013; Legendre et al., 2002). Here geostatistical models are used to quantify the spatial properties of potential indicator species at a long-term deep-water benthic monitoring site, and highlight how these properties influence survey outcomes. Spatial properties of organisms as described by range and spatial variance parameters are found to have an appreciable influence on sampling outcomes. Target organisms that were found to have short effective ranges and high spatial variances require both increased geolocation precision for repeat transects and a higher sampling intensity to achieve high precision outcomes. Through simulations based on model outputs, it was found that 2 m offsets in repeat transects, which are typical for an AUV, are unlikely to have major impacts on the probability of detecting change in indicator species, provided that at least every 50th image (a spacing of approximately 20 m) was systematically sampled along the transect. At a larger offset distance of 10 m, much higher image sampling is likely to be required in order to achieve a high probability of detecting change in the cover of the same species. These findings have important implications for researchers interested in monitoring change in benthic ecosystems, and highlight the importance of considering the interaction between sampling design, the technical limitations of survey equipment and the spatial properties of indicator species.

4.1 The spatial properties of deep-water benthic species

Variability in survey outcomes introduced through the distributional patterns of organisms can have a marked effect on the ability to detect change and therefore should be taken into account when planning monitoring programmes (Legendre et al., 2002; Thrush, Pridmore, & Hewitt, 1994; Tobin, 2004). The geostatistical descriptions of the species in this study provide the first detailed quantitative description of the spatial properties of deep-water benthic species over small scales (1-100s metres). Quantifying spatial properties and their influence on sampling outcomes at this scale is vital for monitoring programmes where there is a need to ensure the precision of site-level survey outcomes. Similar descriptions at this scale are currently limited to terrestrial examples (e.g. Cardina, Johnson, & Sparrow, 1997; Park & Lee, 2014), perhaps due to the sampling effort and computational difficulties associated with spatial modelling of the large data sets required. Novel computational approaches, such as INLA, may provide a remedy to this situation, allowing a growing database of such descriptions for cross-system comparison.

Model outputs showed that many of the species have effective ranges of less than 5 metres indicating spatial dependence within individual patches that are metres in diameter. Studies in shallower marine environments have also emphasized the large variability in individual species abundances between sampling plots at small scales (from centimetres to metres) at a site scale (e.g. Underwood, Chapman, & Connell, 2000; Ysebaert & Herman, 2002). Where indicator species display high levels of spatial autocorrelation over small distances, as indicated by short ranges, it might be expected that spatially precise repeat transects that are relocated within this range distance would be required for precise survey outcomes. These results highlight the necessity of simultaneously considering the spatial properties, repeat geolocation precision of transects and the sampling intensity.

4.2 The importance of repeat transect precision for benthic monitoring

When conducting repeat surveys with the aim of detecting change, surveys should be designed to minimize the variability introduced into the subsequent analysis (Larsen et al., 2001; Urquhart & Kincaid, 1999; van der Meer, 1997). For repeat surveys utilizing transects, it is important to maximize the covariance between repeat observations (in the case of this study, repeat images), by minimizing the distance between the repeat transects (Ryan & Heyward, 2003). The geostatistical analysis conducted here shows that spatially precise repeat transects may increase the repeat precision of estimates of percentage cover for species that have short effective ranges and high spatial variance. Achieving high precision in cover estimates when repeat transects are spatially offset requires an increased amount of sampling that will be dependent on both the offset distance and the spatial properties of the indicators. A high probability of detecting a 50% decrease in percentage cover is shown to be achievable for the majority of species studied with up to a 10 m offset, provided that image sampling levels along the transect are sufficiently high (every 5th image = approximately every 2 m along the transect). At a smaller offset of 2 m, such as may be expected with an AUV, a much reduced sampling intensity can be employed to achieve similar probabilities of detection. Conversely, a smaller decrease in percentage cover can be detected for a small offset with less sampling intensity than would be required with a larger offset. With technologies such as towed video or imaging sleds that are likely to have larger offsets, researchers need to carefully consider whether the level of image sampling needed to achieve precise repeat transects is prohibitive for the indicators in question. Furthermore, difficulty in maintaining constant altitude above the sea floor with platforms such as towed video or imaging sleds (Thresher et al., 2014), may result in an insufficient amount of useable imagery to obtain precise cover estimates.

4.3 The importance of sampling intensity for repeat transects

Variability due to sampling design, such as the number of transects and/or the transect design, the number of images and the number of points within images can have a marked effect on sampling estimates (Brown et al., 2004; Leujak & Ormond, 2007; Molloy et al., 2013). While the repeat precision of transects will be dependent on factors largely outside of a researcher's ability to control, such as the technical limitations of the survey platform and prevailing currents, determining the number of images needed to be sampled is an important consideration to achieve adequate precision without wasting sampling effort. Based on previous research which showed that a large number of images are likely to be required for precise estimates of low cover species such as occur in this study system, it was anticipated there would be a need to sample in excess of 100 images (Perkins et al., 2016). While scoring for continuous coverage along a transect is optimal, the results show that where species are found to have longer ranges and lower spatial variances a reduced sampling effort can be employed. Scoring every 20th image (a total of 156 images at this site) gave >80% probability of detecting a halving in the odds of presence for 17 out of 20 species at a 2 m displacement. This represents a considerable reduction in scoring effort to scoring every 5th image (a total of 622 images), while maintaining a reasonable probability of detecting temporal change.

The final selection of indicators for long-term monitoring will depend on a range of factors specific to the programme (see Hayes et al., 2015). Although the present study has focused only on statistical and logistical considerations, the results suggest that geostatistical analyses may provide a useful tool to help in choosing suitable indicators. For example, if researchers decide that a certain level of image sampling is prohibitively high, then certain indicators can be ruled out as being suitable monitoring candidates due to the difficulty in gaining sufficient precision in estimates of cover. Species with low probability of detecting temporal decline at larger offsets or reduced image sampling were found to be those species that had geostatistical properties of short ranges or high spatial variances or both. Pilot studies that incorporate intense image scoring in the early stages of a monitoring program would allow greater precision in initial cover estimates and model parameters. Such an effort in the early stages of a monitoring program could guide ongoing sampling levels and the narrowing down of potential indicators at a later stage. In addition to aiding in indicator selection, pilot studies would allow cost-benefit analyses of the trade-off of differing sampling designs and/or tool combinations.

Although alternative transect designs were not tested in this study, transect layouts that provide a better coverage of images over the site are likely to provide higher precision in estimates of cover of benthic species (Cole, Healy, Wood, & Foster, 2001; Foster et al., 2014). Previous studies examining sampling of imagery have typically been based on the use of multiple short (< 50 m) transects in shallow-water sites, where more transects are often recommended in order to increase the precision of estimates (e.g. Brown et al., 2004; Molloy et al., 2013; Ryan & Heyward, 2003). In contrast, transect designs for AUVs typically involve multiple grid lines (e.g. Figure 1c), over meso-scales (100s m to kms; Pizarro et al., 2013; Van Rein et al., 2009). Rigby et al. (2014) show through simulation, the sensitivity of model parameter estimates to sample effort when using transect sampling designs. Understanding the trade-off between sampling effort, model parameter estimation, and the effect sizes detectable for ecological monitoring programmes is crucial for effective design. The present analysis shows that by sampling a sufficient number of images with the current grid design transect layout, high probability of detecting a 50% change can be achieved.

Acknowledgements

This work was undertaken for the Marine Biodiversity Hub, a collaborative partnership supported through funding from the Australian Government's National Environmental Science Programme. Our goal is to assist decision-makers to understand, manage and conserve Australia's environment by funding world-class biodiversity science.

References

Abramowitz, M., & Stegun, I. (1972). *Handbook of mathematical functions*: Courier Dover Publications.

Althaus, F., Hill, N. A., Rees, R., Jordan, A., & Colquhuon, J. (2013). CATAMI Standardised Classification Scheme Visual look-up guide. In L. Edwards (Ed.), Collaborative and Automative Tools for Marine Imagery (CATAMI).

Andrew, N. L., & Mapstone, B. D. (1987). Sampling and the description of spatial pattern in marine ecology. *Oceanography and Marine Biology, 25*, 39-90.

Babcock, R. C., Shears, N. T., Alcala, A. C., Barrett, N. S., Edgar, G. J., Lafferty, K. D., . . . Russ, G. R. (2010). Decadal trends in marine reserves reveal differential rates of change in direct and indirect effects. *Proc Natl Acad Sci U S A, 107*(43), 18256-18261. doi:10.1073/pnas.0908012107

Banerjee, S., Carlin, B. P., & Gelfand, A. E. (2004). *Hierarchical modeling and analysis for spatial data*: Chapman and Hall/CRC

Barry, S., & Elith, J. (2006). Error and uncertainty in habitat models. *Journal of Applied Ecology, 43*(3), 413-423. doi:10.1111/j.1365-2664.2006.01136.x

Beijbom, O., Edmunds, P. J., Roelfsema, C., Smith, J., Kline, D. I., Neal, B. P., . . . Kriegman, D. (2015). Towards Automated Annotation of Benthic Survey Images: Variability of Human Experts and Operational Modes of Automation. *Plos One, 10*(7), e0130312. doi:10.1371/journal.pone.0130312

Blangiardo, M., & Cameletti, M. (2015). *Spatial and spatio-temporal Bayesian models with R-INLA*: Wiley.

Boavida, J., Assis, J., Reed, J., Serrão, E. A., & Gonçalves, J. M. S. (2015). Comparison of small remotely operated vehicles and diver-operated video of circalittoral benthos. *Hydrobiologia, 766*(1), 247-260. doi:10.1007/s10750-015-2459-y

Brind'Amour, A., Laffargue, P., Morin, J., Vaz, S., Foveau, A., & Le Bris, H. (2014). Morphospecies and taxonomic sufficiency of benthic megafauna in scientific bottom trawl surveys. *Continental Shelf Research, 72*, 1-9. doi:10.1016/j.csr.2013.10.015

Brown, C. J., Schoeman, D. S., Sydeman, W. J., Brander, K., Buckley, L. B., Burrows, M., . . . Richardson, A. J. (2011). Quantitative approaches in climate change ecology. *Global Change Biology, 17*(12), 3697-3713. doi:10.1111/j.1365-2486.2011.02531.x

Brown, E., Cox, E., Jokiel, P., Rodgers, K., Smith, W., Tissot, B., . . . Hultquist, J. (2004). Development of benthic sampling methods for the Coral Reef Assessment and Monitoring Program (CRAMP) in Hawai'i. *Pacific Science, 58*(2), 145-158.

Cardina, J., Johnson, G. A., & Sparrow, D. H. (1997). The nature and consequence of weed spatial distribution. *Weed Science, 45*(3), 364-373.

Chu, J. W. F., & Leys, S. P. (2010). High resolution mapping of community structure in three glass sponge reefs (Porifera, Hexactinellida). *Marine Ecology Progress Series, 417*, 97-113. doi:10.3354/meps08794

Cole, R. G., Healy, T. R., Wood, M. L., & Foster, D. M. (2001). Statistical analysis of spatial pattern: A comparison of grid and hierarchical sampling approaches. *Environmental Monitoring and Assessment, 69*(1), 85-99. doi:Doi 10.1023/A:1010756729485

Diggle, P. J., & Ribeiro, P. J. (2007). *Model-based Geostatistics*. New York: Springer-Verlag.

Elston, D. A., Nevison, I. M., Scott, W. A., Sier, A. R. J., & Morecroft, M. D. (2011). Power calculations for monitoring studies: a case study with alternative models for random variation. *Environmetrics, 22*(5), 618-625. doi:10.1002/env.1096

Foster, S. D., Hosack, G. R., Hill, N. A., Barrett, N. S., Lucieer, V. L., & Spencer, M. (2014). Choosing between strategies for designing surveys: autonomous underwater vehicles. *Methods in Ecology and Evolution, 5*(3), 287-297. doi:10.1111/2041-210x.12156

Halpern, B. S., Walbridge, S., Selkoe, K. A., Kappel, C. V., Micheli, F., D'Agrosa, C., . . . Watson, R. (2008). A global map of human impact on marine ecosystems. *Science, 319*, 948-952.

Hayes, K. R., Dambacher, J. M., Hosack, G. R., Bax, N. J., Dunstan, P. K., Fulton, E., . . . Marshall, C. M. (2015). Identifying indicators and essential variables for marine ecosystems. *Ecological Indicators, 57*, 409-419.

Horne, J. K., & Schneider, D. C. (1995). Spatial Variance in Ecology *Oikos, 74*, 18-26.

Hughes, T. P., Bellwood, D. R., Folke, C., Steneck, R. S., & Wilson, J. (2005). New paradigms for supporting the resilience of marine ecosystems. *Trends Ecol Evol, 20*(7), 380-386. doi:10.1016/j.tree.2005.03.022

Huvenne, V. A. I., Bett, B. J., Masson, D. G., Le Bas, T. P., & Wheeler, A. J. (2016). Effectiveness of a deep-sea cold-water coral Marine Protected Area, following eight years of fisheries closure. *Biological Conservation, 200*, 60-69. doi:10.1016/j.biocon.2016.05.030

Irvine, K. M., Thornton, J., Backus, V. M., Hohmann, M. G., Lehnhoff, E. A., Maxwell, B. D., . . . Rew, L. J. (2013). A comparison of adaptive sampling designs and binary spatial models : a simulation study using a census ofBromus inermis. *Environmetrics*, n/a-n/a. doi:10.1002/env.2223

James, L. C., Marzloff, M. P., Barrett, N., Friedman, A., & Johnson, C. R. (2017). Changes in deep reef benthic community composition across a latitudinal and environmental gradient in temperate Eastern Australia. *Marine Ecology Progress Series, (forthcoming)*.

Karpov, K. A., Bergen, M., & Geibel, J. J. (2012). Monitoring fish in California Channel Islands marine protected areas with a remotely operated vehicle: the first five years. *Marine Ecology Progress Series, 453*, 159-172. doi:10.3354/meps09629

Larsen, D. P., Kincaid, T. M., Jacobs, S. E., & Urquhart, N. S. (2001). Designs for evaluating local and regional scale trends. *BioScience, 51*(12), 1069-1078. doi:Doi 10.1641/0006-3568(2001)051[1069:Dfelar]2.0.Co;2

Legendre, P. (1993). Spatial Autocorrelation: Trouble or New Paradigm? *Ecology, 74*(6), 1659-1673.

Legendre, P., Dale, M. R. T., Fortin, M. J., Gurevitch, J., Hohn, M., & Myers, D. (2002). The consequences of spatial structure for the design and analysis of ecological field surveys. *Ecography, 25*(5), 601-615. doi:DOI 10.1034/j.1600-0587.2002.250508.x

Leujak, W., & Ormond, R. F. G. (2007). Comparative accuracy and efficiency of six coral community survey methods. *Journal of Experimental Marine Biology and Ecology, 351*(1-2), 168-187. doi:DOI 10.1016/j.jembe.2007.06.028

Lindgren, F., Rue, H., & Lindstrom, J. (2011). An explicit link between Gaussian fields and Gaussian Markov random fields: the stochastic partial differential equation approach. *Journal of the Royal Statistical Society Series B-Statistical Methodology, 73*, 423-498. doi:10.1111/j.1467-9868.2011.00777.x

Molloy, P. P., Evanson, M., Nellas, A. C., Rist, J. L., Marcus, J. E., Koldewey, H. J., & Vincent, A. C. J. (2013). How much sampling does it take to detect trends in coral-reef habitat using photoquadrat surveys? *Aquatic conservation: marine and freshwater ecosystems, 23*(6), 820-837. doi:10.1002/aqc.2372

Monk, J., Barrett, N. S., Hill, N. A., Lucieer, V. L., Nichol, S. L., Siwabessy, P. J. W., & Williams, S. (2016). Outcropping reef ledges drive patterns of epibenthic assemblage diversity on cross-shelf habitats. *Biodiversity and Conservation, 25*(3), 485-502.

Park, J. S., & Lee, E. J. (2014). Geostatistical analyses and spatial distribution patterns of tundra vegetation in Council, Alaska. *Journal of Ecology and Environment, 37*(2), 53-60. doi:10.5141/ecoenv.2014.007

Parmesan, C., Duarte, C., Poloczanska, E., Richardson, A. J., & Singer, M. C. (2011). COMMENTARY: Overstretching attribution. *Nature climate change, 1*(1), 2-4.

Perkins, N. R., Foster, S. D., Hill, N. A., & Barrett, N. S. (2016). Image subsampling and point scoring approaches for large-scale marine benthic monitoring programs *Estuarine Coastal and Shelf Science, 176*, 36-46. doi:doi:10.1016/j.ecss.2016.04.005

Perkins, N. R., Foster, S. D., Hill, N. A., Marzloff, M. P., & Barrett, N. S. (2017). Temporal and spatial variability in the cover of deep reef species: Implications for monitoring. *Ecological Indicators, 77*, 337-347. doi:10.1016/j.ecolind.2017.02.030

Pizarro, O., Williams, S. B., Jakuba, M. V., Johnson-Roberson, M., Mahon, I., Bryson, M., . . . Douillard, B. (2013). *Benthic monitoring with robotic platforms-The experience of Australia*, Tokyo.

Rigby, P., Pizarro, O., & Williams, S. (2014). Estimation of Clustering Parameters Using Gaussian Process Regression. *Plos One, 9*(11). doi:10.1371/

Rue, H., Martino, S., & Chopin, N. (2009). Approximate Bayesian Inference for Latent Gaussian Models by Using Integrated Nested Laplace Approximations. *Journal of the Royal Statistical Society, 71*(2), 319-392.

Ryan, D. A. J., & Heyward, A. (2003). Improving the precision of longitudinal ecological surveys using precisely defined observational units. *Environmetrics, 14*(3), 283-293. doi:10.1002/env.586

Schlacher, T. A., Schlacher-Hoenlinger, M. A., Williams, A., Althaus, F., Hooper, J. N. A., & Kloser, R. (2007). Richness and distribution of sponge megabenthos in continental margin canyons off southeastern Australia. *Marine Ecology Progress Series, 340*, 73-88. doi:DOI 10.3354/meps340073

Schlacher, T. A., Williams, A., Althaus, F., & Schlacher-Hoenlinger, M. A. (2010). High-resolution seabed imagery as a tool for biodiversity conservation planning on continental margins. *Marine Ecology, 31*(1), 200-221. doi:10.1111/j.1439-0485.2009.00286.x

Shepherd, S., & Edgar, G. J. (2013). *Ecology of Australian temperate reefs : the unique south* (S. Shepherd & G. J. Edgar Eds.). Collingwood, Victoria: CSIRO Publishing.

Skalski, J. R. (2012). Estimating variance components and related parameters when planning long-term monitoring programs. In R. A. Gitzen, J. J. Millspaugh, A. B. Cooper, & D. S. Licht (Eds.), *Design and Analysis of Long-term Ecological Monitoring Studies* (pp. 174-199): Cambridge University Press.

Thresher, R., Althaus, F., Adkins, J., Gowlett-Holmes, K., Alderslade, P., Dowdney, J., . . . Williams, A. (2014). Strong depth-related zonation of megabenthos on a rocky continental margin (approximately 700-4000 m) off southern Tasmania, Australia. *Plos One, 9*(1), e85872. doi:10.1371/journal.pone.0085872

Thrush, S. F., Pridmore, R. D., & Hewitt, J. E. (1994). Impacts on Soft-Sediment Macrofauna - the Effects of Spatial Variation on Temporal Trends. *Ecological Applications, 4*(1), 31-41. doi:Doi 10.2307/1942112

Tobin, P. C. (2004). Estimation of the Spatial Autocorrelation Function: Consequences of Sampling Dynamic Populations in Space and Time. *Ecography, 27*(6), 767-775.

Underwood, A. J., Chapman, M. G., & Connell, S. D. (2000). Observations in ecology: you can't make progress on processes without understanding the patterns. *Journal of Experimental Marine Biology and Ecology, 250*.

Urquhart, N. S., & Kincaid, T. M. (1999). Designs for detecting trend from repeated surveys of ecological resources. *Journal of Agricultural, Biological, and Environmental Statistics, 4*(4), 404 - 414.

Urquhart, N. S., Overton, W. S., & Birkes, D. S. (1993). Comparing sampling designs for monitoring ecological status and trends: Impact of temporal patterns. In *Statistics for the environment* (pp. 71-85). Lisbon, Portugal: Wiley.

van der Meer, J. (1997). Sampling design of monitoring programmes for marine benthos: a comparison between the use of fixed versus randomly selected stations. *Journal of Sea Research, 37*, 167-179.

Van Rein, H. B., Brown, C. J., Quinn, R., & Breen, J. (2009). A review of sublittoral monitoring methods in temperate waters: a focus on scale. *Underwater Technology, 28*(3), 99-113. doi:10.3723/ut.28.099

Whiteman, L., Meyer, E., Freidenburg, T., Rindge, H., Meyer, R., Pribyl, A., . . . (Eds), T. M. (2013). *State of the California Central Coast: Results from Baseline Monitoring of Marine Protected Areas 2007–2012*. Retrieved from California, USA:

Williams, A., Althaus, F., Barker, B., Kloser, R., & Keith, G. (2007). *Research and monitoring for benthic ecosysytems in Marine Protected Areas of the South East Marine Region (SEMR)*. Retrieved from Hobart, Tasmania:

Williams, A., Althaus, F., & Schlacher, T. A. (2015). Towed camera imagery and benthic sled catches provide different views of seamount benthic diversity. *Limnology and Oceanography: Methods, 13*(2), 62-73. doi:10.1002/lom3.10007

Williams, S. B., Pizarro, O. R., Jakuba, M. V., Johnson, C. R., Barrett, N. S., Babcock, R. C., . . . Friedman, A. (2012). Monitoring of Benthic Reference Sites Using an Autonomous Underwater Vehicle. *Ieee Robotics & Automation Magazine, 19*(1), 73-84. doi:Doi 10.1109/Mra.2011.2181772

Ysebaert, T., & Herman, P. M. J. (2002). Spatial and temporal variation in benthic macrofauna and relationships with environmental variables in an estuarine, intertidal soft-sediment environment. *Marine Ecology Progress Series, 244*, 105-124. doi:DOI 10.3354/meps244105

Table 1: Summary of model outputs based on the original scored data for all 20 species. Mean effective range and spatial variances are the mean of the posterior distribution from the INLA models. Species classifications are based on the CATAMI system (see Althaus, Hill, Rees, Jordan, & Colquhuon, 2013).

Species	**Percent Cover (%)**	**Number of images present (Total = 622)**	**Mean spatial variance**	**Mean effective range (m)**
Bryozoan sp.	0.09	23 (4%)	3.28	45.41
Gorgonian sp.	1.4469	246 (40%)	1.33	16.57
Black coral sp.	0.1736	21 (3%)	13.4	3.37
Erect sponge sp. 1	0.2797	48 (8%)	5.2	3.09
Erect sponge sp. 2	0.5241	112 (18%)	1.19	4.37
Erect sponge sp. 3	0.9711	162 (26%)	1.71	3.38
Laminar sponge sp. 1	0.2476	44 (7%)	4.81	5.67
Laminar sponge sp. 2	0.0193	4 (< 1%)	0.54	103.12
Laminar sponge sp. 3	0.0129	3 (<1%)	2.57	94.33
Palmate sponge sp.	0.0932	19 (3%)	5.5	20.56
Cup sponge sp. 1	0.2219	40 (6%)	5.09	2.65
Cup sponge sp. 2	0.1994	38 (6%)	5.54	2.39
Cup sponge sp. 3	0.3826	77 (12%)	2.87	2.37
Cup sponge sp. 4	0.5241	87 (14%)	4.28	2.3
Cup sponge sp. 5	0.119	23 (4%)	10.37	23.43
Cup sponge sp. 6	0.3215	71 (11%)	2.26	3.46
Massive sponge sp. 1	0.6174	122 (20%)	1.82	3.51
Massive sponge sp. 2	0.1897	42 (7%)	2.82	3.93
Massive sponge sp. 3	0.4084	82 (13%)	1.97	9.75
Massive sponge sp. 4	0.0032	1 (< 1%)	0.14	114.27

Figure 1: The study site, showing (A) the regional setting, (B) the transect location, and (C) the transect used for scoring with an underlying multibeam sonar map showing the location of reef and the depth profile. Blue shaded area indicates the Commonwealth Marine Reserve boundaries.

Figure 2: Posterior distribution of the range for all 20 species. Each line represents the posterior distribution of the range for one of the 20 species. The range has been truncated at 100 metres, as this covered the mode of the distribution for all species, although values did extend to 2500 m.

Figure 3: Covers of each species in the original scored data, and biases and credible intervals in offset transects scored with every 5th image: **(a)** Distribution of empirical data for the six chosen species across the transect. Grey lines show AUV flight path. Circle sizes reflect relative percent covers within images along the original transect as indicated by the scale at the bottom **(b)** Mean difference (i.e. bias) and 95% credible intervals for percent cover estimates between transects conducted along the original locations, compared to offset transects. Offset distances have been truncated to 32 m to allow better resolution of small offsets. Dashed line is at zero, indicating zero bias between original and offset transects.

Figure 4: Difference in coefficient of variation (delta CV) for the cover estimate for a transect in the original location, and offset transects at displacements from 0.5 to 32 metres for six species over all simulations. A truncated distance of 32 m was used to improve the resolution at shorter distances. CVs were taken over 5000 simulations, based on 5000

posterior sample draws of the hyperparameters from the INLA models for each species. All scoring was done with every 5th image systematically selected along the transect. The line for Laminar sponge sp. 2 has been truncated to maintain the detail in the other species.

Figure 5: The effect of offset transect displacement distance in combination with different image sampling intensities on the precision of repeat transects for six species. Precision is represented as the difference in coefficient of variation (delta CV) of the mean percent cover estimate from a transect in the original location with every 5th image, and mean percent cover from offset transects at various displacements and with varying image sampling intensities. Note that colours are not consistent between plots. CVs were taken over 5000 simulations.

Figure 6: Probability of detecting a halving in the odds of presence for six species with repeat transects and different image sampling intensities at **(a)** a 2 meter offset distance and **(b)** a 10 m offset distance. Dashed line is at 80% probability of detection.

Appendix – Bayesian priors for the INLA models

In Bayesian statistics, the term 'hyperparameter' refers to a parameter of a prior distribution, which defines a probability distribution based on previous knowledge. Therefore, ecologically meaningful hyperparameters needed to be specified for the following priors: the intercept (α_c), which represent the mean cover over the site; the spatial variance (σ^2); and κ which is related to the range by $r = \sqrt{8\lambda}/\kappa$. The prior specified for ρ_c(equation (5)) induces a prior on κ.The covariance function used was the Matérn covariance function as given by Lindgren et al. (2011):

$$Cov\left(\xi(s_i), \xi(s_j)\right) = \frac{\sigma^2}{\Gamma(\lambda)2^{\lambda-1}}\left(\kappa \parallel s_i - s_j \parallel\right)^{\lambda} \mathrm{K}_{\lambda}\left(\kappa \parallel s_i - s_j \parallel\right),$$

where $\parallel s_i - s_j \parallel$ is the Euclidean distance between two image locations $s_i, s_j \in \mathbb{R}^d$, σ^2 is the marginal variance, and κ is a scaling parameter related to the range r by the relationship $r = \sqrt{8\lambda}/\kappa$ (Lindgren et al., 2011). The term K_{λ} denotes the modified Bessel function of the second kind (Abramowitz & Stegun, 1972). The parameter λ measures the smoothness of the correlation process (Lindgren et al., 2011). A default value of $\lambda = 1$ was used, as this parameter typically has poor identifiability (Blangiardo & Cameletti, 2015) and so its choice has little bearing on the model's interpretation.

Due to the difficulties with surveying waters beyond SCUBA depths, published knowledge regarding the distributional properties of species at these depths is inherently limited. Evidence from surveys from south-east Australia (Schlacher et al., 2007) and Canada (Chu & Leys, 2010), suggests that deep-sea sponge groups are likely to have an effective range (defined as the distance needed before two locations have modelled correlation less than about 0.1, Lindgren *et al.* 2011) on the order of metres to tens of metres. In the absence of detailed information to inform priors for each species separately, priors for the range, intercept and spatial variance were common across all species.

For the range, a normal prior was specified for $\log\rho_c$ such that $P(\rho_c < 100) = P(\rho_c > 30) = 1/4$, which gives an a priori 50% chance that the effective range is between 30 and 100 metres. For the intercept, as previous research (see Perkins et al., 2016) suggested that the majority of deep-water invertebrates have relatively low percent cover (typically less than 5%), a log-normal prior was specified for α_c such that $P(\alpha_c < 0.001) = P(\alpha_c > 0.05) = 1/4$, which gives a 50% chance that the intercept for any given species is between 0.1% and 5%.

Specifying the prior for the marginal spatial variance is more difficult. In particular, the spatial random effects induce dependence at the level of the linear predictor rather than the observations. The prior is developed for images located far enough apart that spatial dependence is negligible. Let the mean percent cover for species c be defined by the intercept α_c such that,

$$\pi_c = \frac{\exp\alpha_c}{(1+\exp\alpha_c)}$$

Then the prior Eq. (6) induces a normal prior on the log odds ratio of the percent cover at location s_i relative to the average,

$$\log R(s_i, c) = \log\left(\frac{p(s_i, c)}{1-\ p(s_i, c)}\right) - \log\left(\frac{\pi_c}{1-\ \pi_c}\right) \sim N(0, \sigma_c^2),$$

where $\log\left(\frac{\pi_c}{1-\pi_c}\right) = \alpha_c$. This implies a lognormal prior on the odds ratio $R(s_i, c) = (p(s_i, c)/(1 - p(s_i, c)))/(\pi_c/(1-\ \pi_c))$. If $\sigma_c = 0.421$ then the probability that this odds ratio exceeds 1/2 or 2 is given by, $P(R(s_i, c)) < 1/2 \ \cup R(s_i, c) > 2) = 0.10$. Similarly, if σ_c

= 1.400 then the probability that this odds ratio exceeds 1/10 or 10 is given by, $P(R(s_i, c)) < 1/10 \cup R(s_i, c) > 10)$ = 0.100. A normal prior for log σ_c with hyperparameters a_σ = -0.264 and b_σ = 0.890 (the mean and standard deviation, respectively) was chosen such that $P(\sigma_c < 0.421) = P(\sigma_c > 1.4) = 0.25$, which gives a 50% chance that the spatial standard deviation is between the above two bounds.

Supplementary Materials – Results for remaining 14 species

Bryozoan sp.

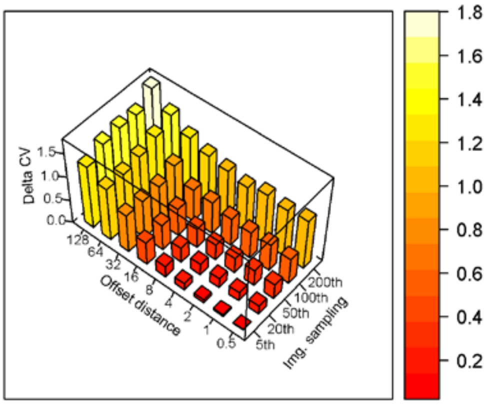

Erect sponge sp. 2

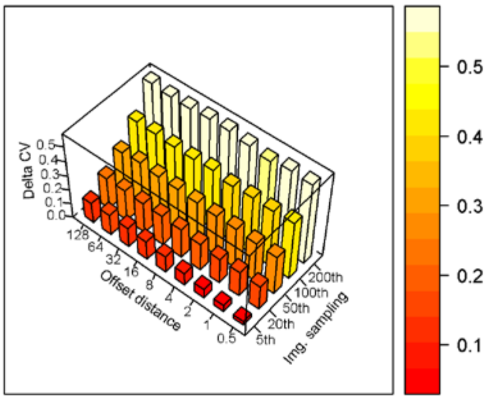

Laminar sponge sp. 1

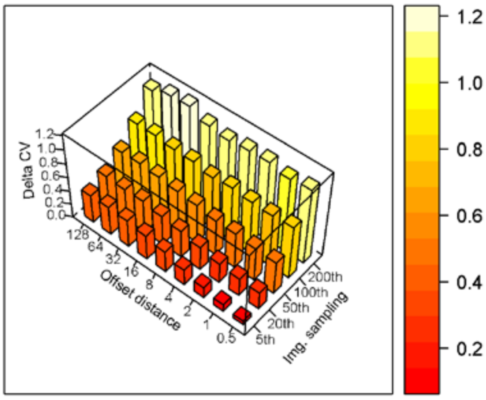

Laminar sponge sp. 3

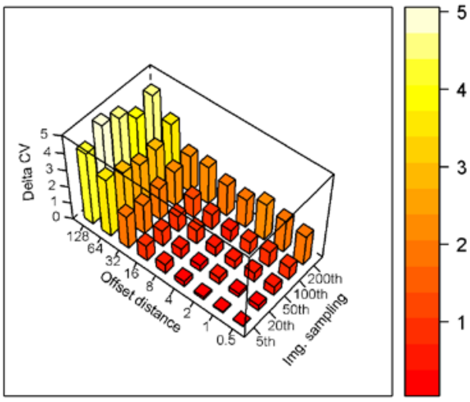

Palmate sponge sp.

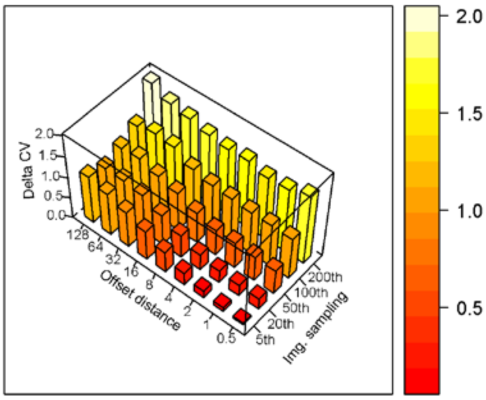

Cup sponge sp. 1

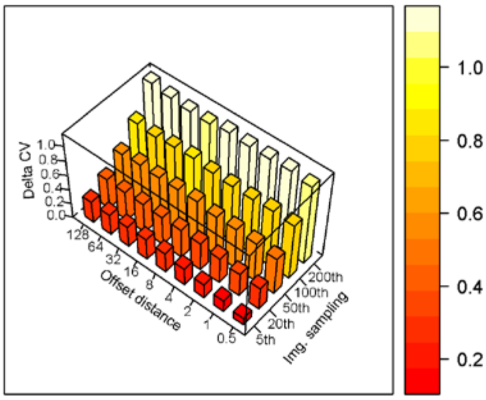

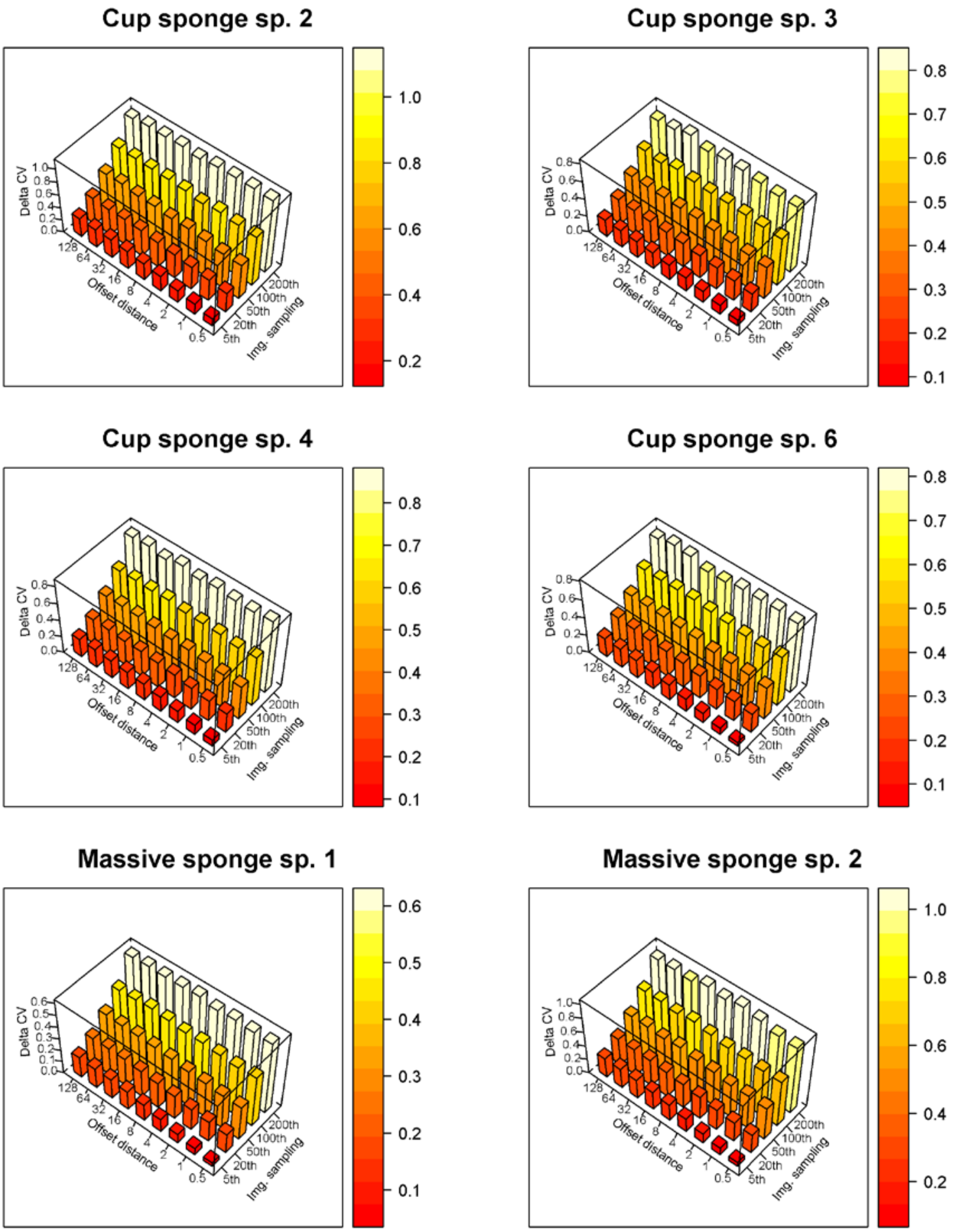
Cup sponge sp. 2
Cup sponge sp. 3
Cup sponge sp. 4
Cup sponge sp. 6
Massive sponge sp. 1
Massive sponge sp. 2
Delta CV
Offset distance
128
64
32
16
8
4
2
1
0.5
Img. sampling
200th
100th
50th
20th
5th

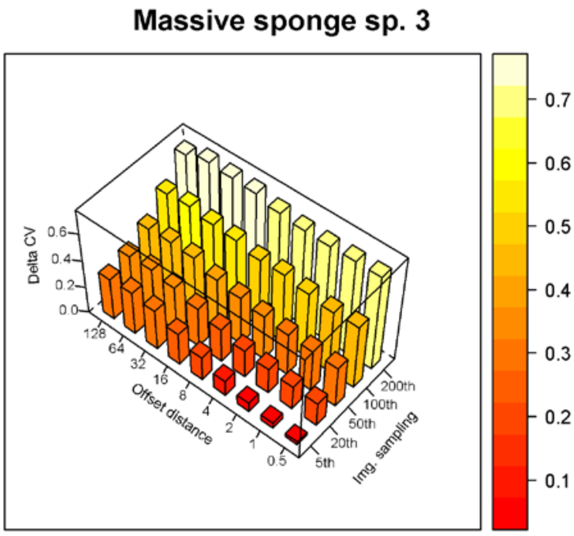

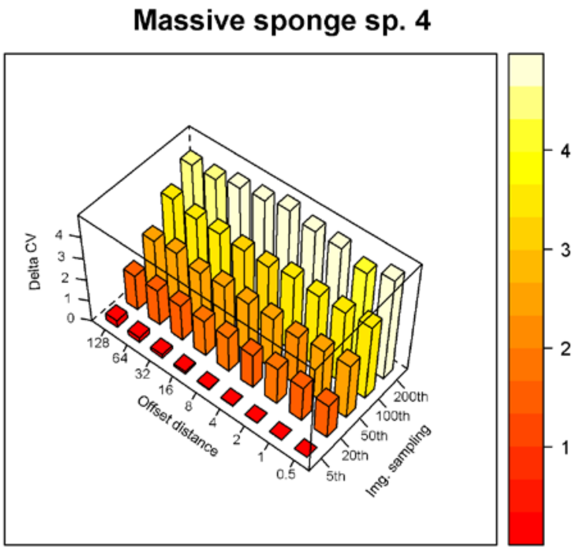

Fig. S1: Difference in coefficients of variation (CVs) of the percent cover estimate for a transect in the original location, and offset transects at various displacements and with varying image sampling intensities for the remaining fourteen species in the study (see Fig. 5). CVs were taken over 1000 simulations, based on 1000 posterior sample draws of the parameters from the INLA models.

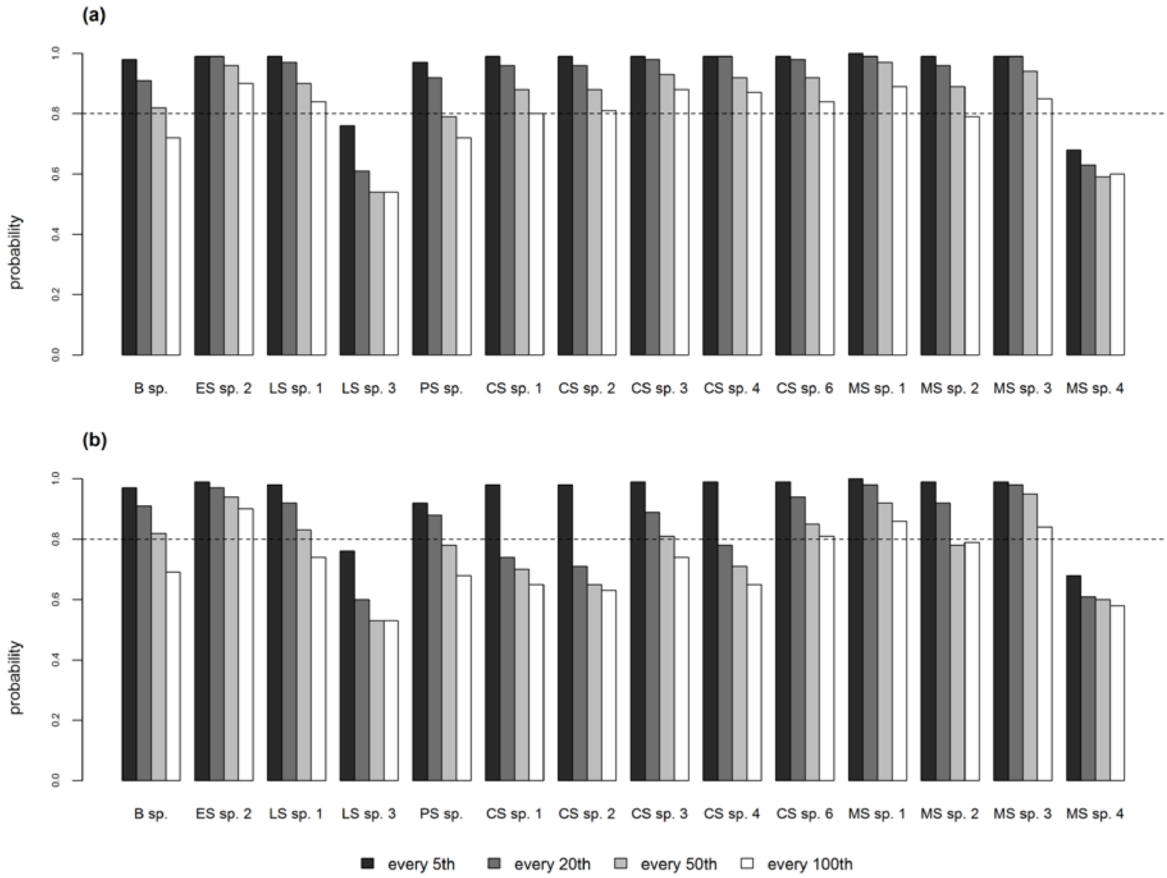

Fig. S2: Probability to detect a decrease given a 50% decrease in the odds of presence for the 14 remaining species in the study (see Fig. 6) with repeat transects and differing image sampling intensities at **(a)** a 2 metre offset distance and **(b)** a 10 m offset distance. Dashed line is at 0.8 probability. B = Bryozoan, ES = Erect sponge, LS = Laminar sponge, CS = Cup sponge, MS = Massive sponge.

Supplementary Material – Species Catalogue

Sample Images	Broad Taxonomic Group	Specifier	Shape	Colour	Species
	Bryozoan		Soft	Brown	Bryozoan sp.
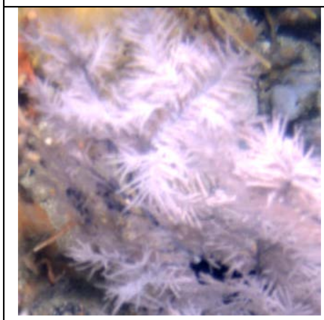	Cnidarian	Black Coral	3D Branching – Bottlebrush	White	Black coral sp.
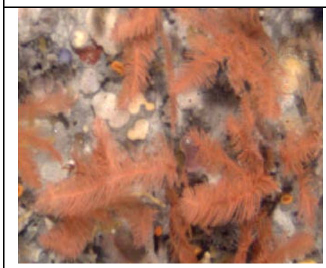	Cnidarian	Gorgonian	Soft – Fern Frond	Orange / Red	Gorgonian sp.
	Sponge	Branching	Thick	Grey / Purple	Erect sponge sp. 3

	Sponge	Branching	Thick	Orange	Erect sponge sp. 2
	Sponge	Branching		Brown	Erect sponge sp. 1
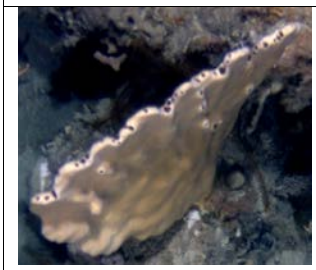	Sponge	Laminar	Top Osicles	Grey / Peach	Laminar sponge sp. 1
	Sponge	Laminar	Top Osicles	Orange	Laminar sponge sp. 2
	Sponge	Laminar	Side Osicles / Flat	Orange	Laminar sponge sp. 3

	Sponge	Palmate	N/A	Orange	Palmate sponge sp.
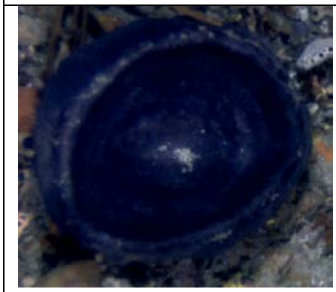	Sponge	Cup	Thick	Blue	Cup sponge sp. 1
	Sponge	Cup	Frilly		Cup sponge sp. 2
	Sponge	Cup	Thick	Grey / Pink	Cup sponge sp. 3
	Sponge	Cup	Thick	Purple / Maroon	Cup sponge sp. 4

	Sponge	Cup	Thick	Red	Cup sponge sp. 5
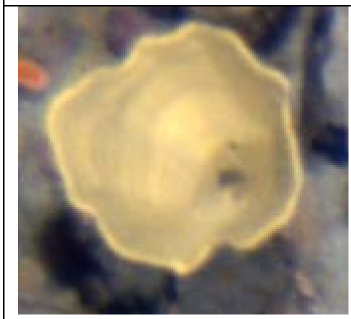	Sponge	Cup	Thin	Yellow	Cup sponge sp. 6
	Sponge	Massive	Papillate	Yellow	Massive sponge sp. 1
	Sponge	Massive	Conc. Osicles	Pink	Massive sponge sp. 2
	Sponge	Massive	Conc. Osicles	Purple	Massive sponge sp. 3

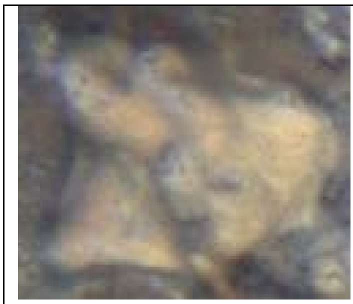	Sponge	Massive	Shapeless	Orange	Massive sponge sp. 4

Supplementary Material – INLA Code

```
# Disclaimer: this is experimental code, designed to be used for one study.
# It is included here as others may find it useful, but we do not necessarily recommend using it as a
# template for future studies

# Note: Users will need to first define the mesh for the study region, and Bayesian priors for:
# spatial range (a.rho and b.rho.prec) and spatial variance (a.sigma and b.sigma.prec) for the
selected species

spde <- inla.spde2.matern(mesh = mesh.b ,
                B.tau = matrix(c(0, -1, +1), nrow = 1, ncol = 3),
                B.kappa = matrix(c(0, 0, -1), nrow = 1, ncol = 3),
                theta.prior.mean = c(a.sigma, a.rho),
                theta.prior.prec = c(b.sigma.prec, b.rho.prec)
                )

# Create a sparse weight matrix 'A' by identifying the data locations in the mesh and organising the
corresponding
# values of the basis functions. sp$utm.x and sp$utm.y define the xy locations for a given species
A <- inla.spde.make.A(mesh = mesh.b, loc = cbind( sp$utm.x, sp$utm.y))

# Define the linear predictor, removing the default intercept and replacing with the object
"intercept"
# 'nodes' define the index for the vertices of the mesh for calculating the spatial random effect
# that is defined by the spde model
formula <- z ~ intercept + f(nodes, model = spde) - 1
```

```
sp$ntrial <- sp$present + sp$absent #define binomial trials for number of points falling on the given species
i.index <- inla.spde.make.index(name = "nodes", n.spde = spde$n.spde) #define an index for the nodes
#Combine data into an inla.stack object
stack <- inla.stack(data=list(z=sp$present,ntrial=sp$ntrial), A=list(A), effects=list(c(i.index, list(intercept=1))))
#fit the model
result <- inla(formula, data=inla.stack.data(stack), control.predictor=list(A=inla.stack.A(stack)), control.inla = list(int.strategy = "grid", dz = 0.2), control.compute=list(config=TRUE), family="binomial", Ntrials=ntrial)
```

Figure 1

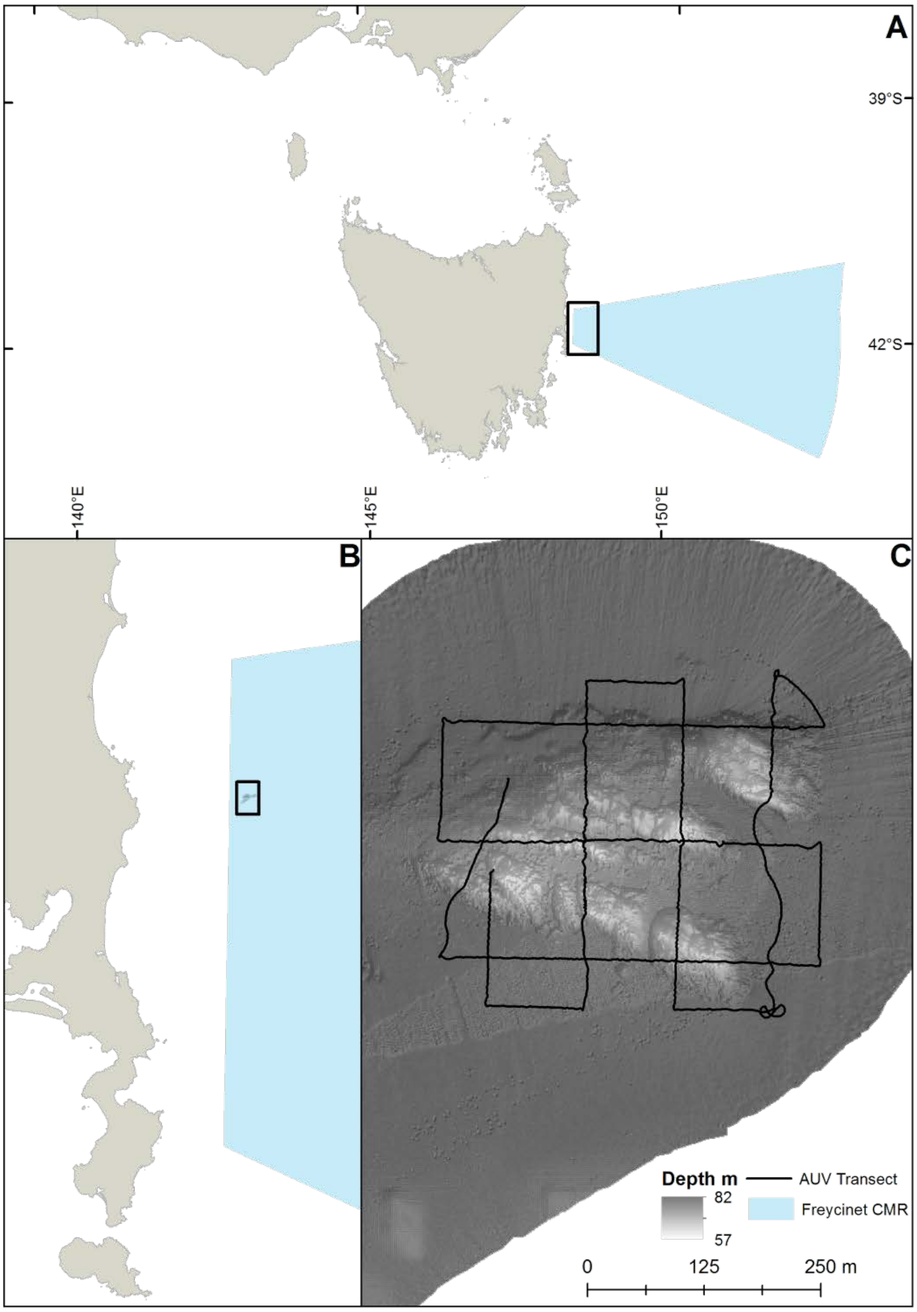
A
39°S
42°S
140°E
145°E
150°E
B
C
Depth m
82
57
AUV Transect
Freycinet CMR
0
125
250 m

Figure 2

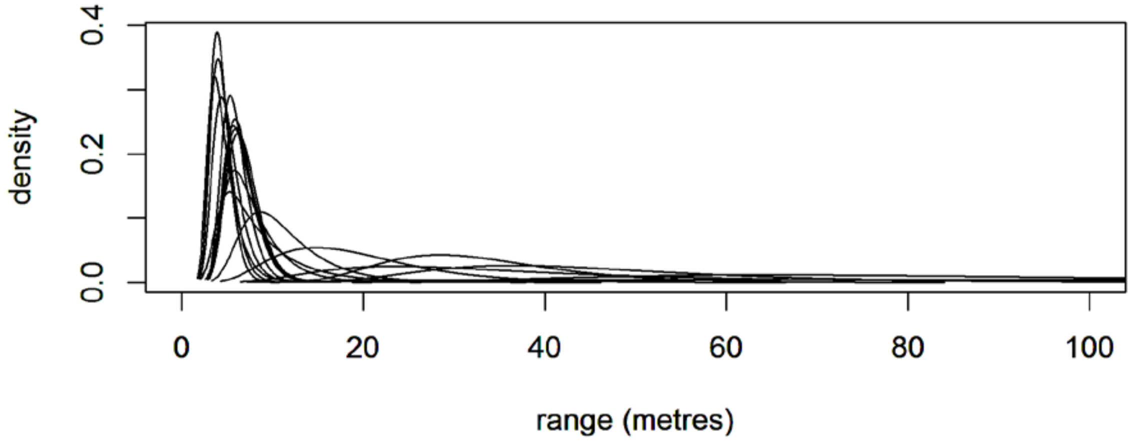

Figure 3

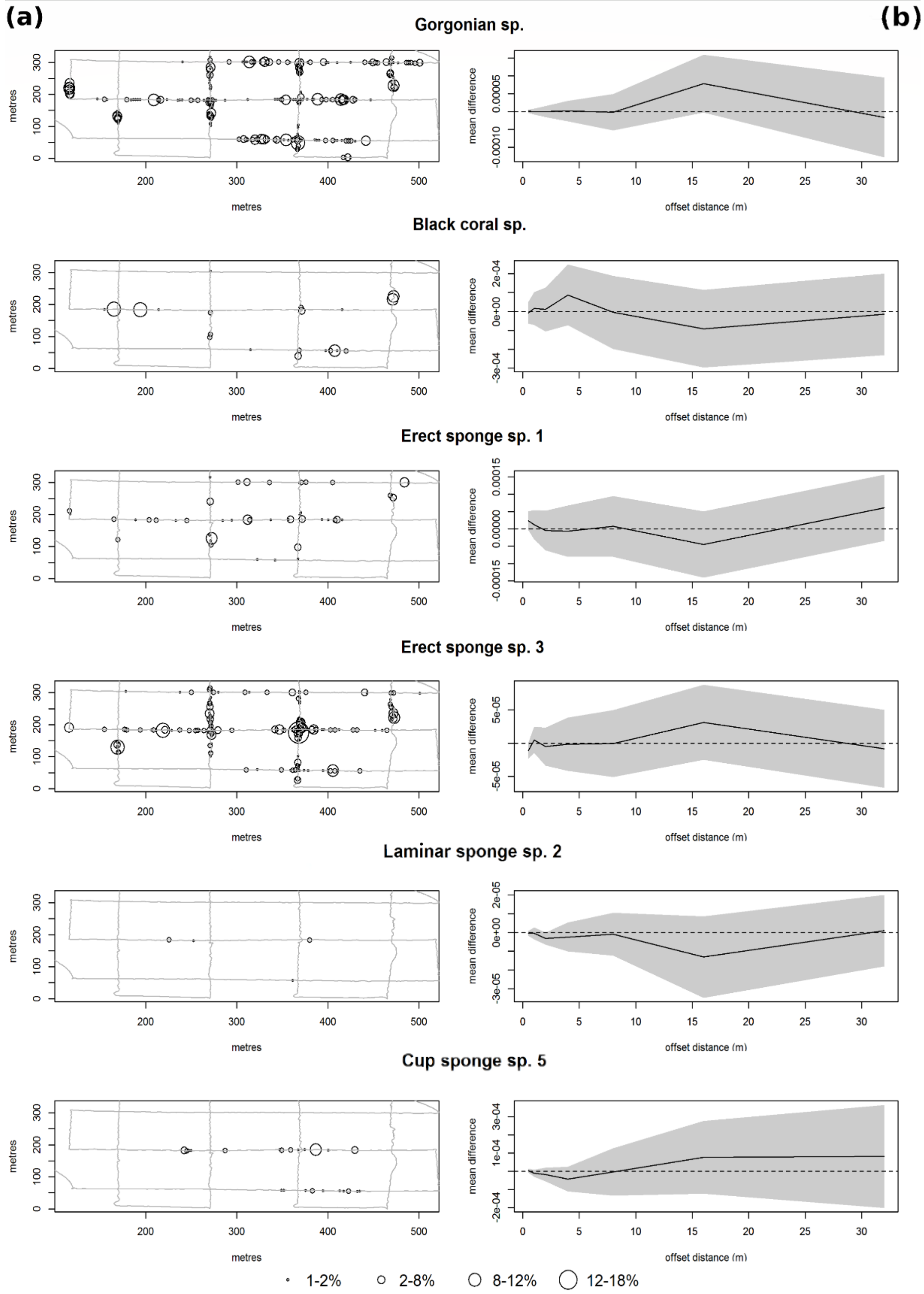
(a)
(b)
Gorgonian sp.
Black coral sp.
Erect sponge sp. 1
Erect sponge sp. 3
Laminar sponge sp. 2
Cup sponge sp. 5
metres
mean difference
offset distance (m)
1-2%
2-8%
8-12%
12-18%

Figure 4

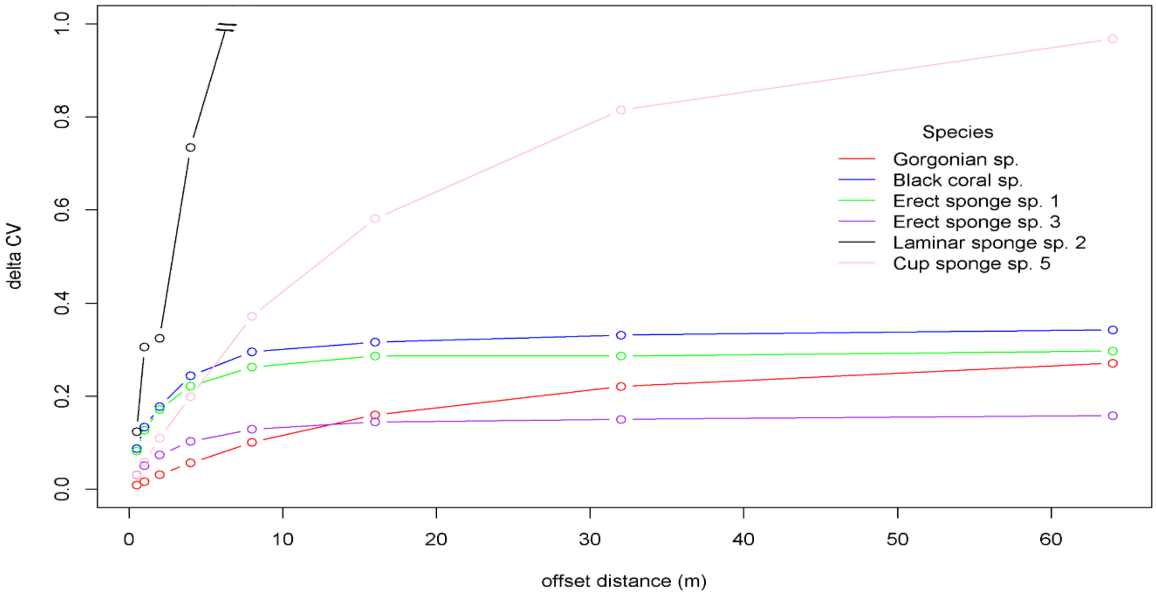
delta CV
0.0
0.2
0.4
0.6
0.8
1.0
0
10
20
30
40
50
60
offset distance (m)
Species
Gorgonian sp.
Black coral sp.
Erect sponge sp. 1
Erect sponge sp. 3
Laminar sponge sp. 2
Cup sponge sp. 5

Figure 5

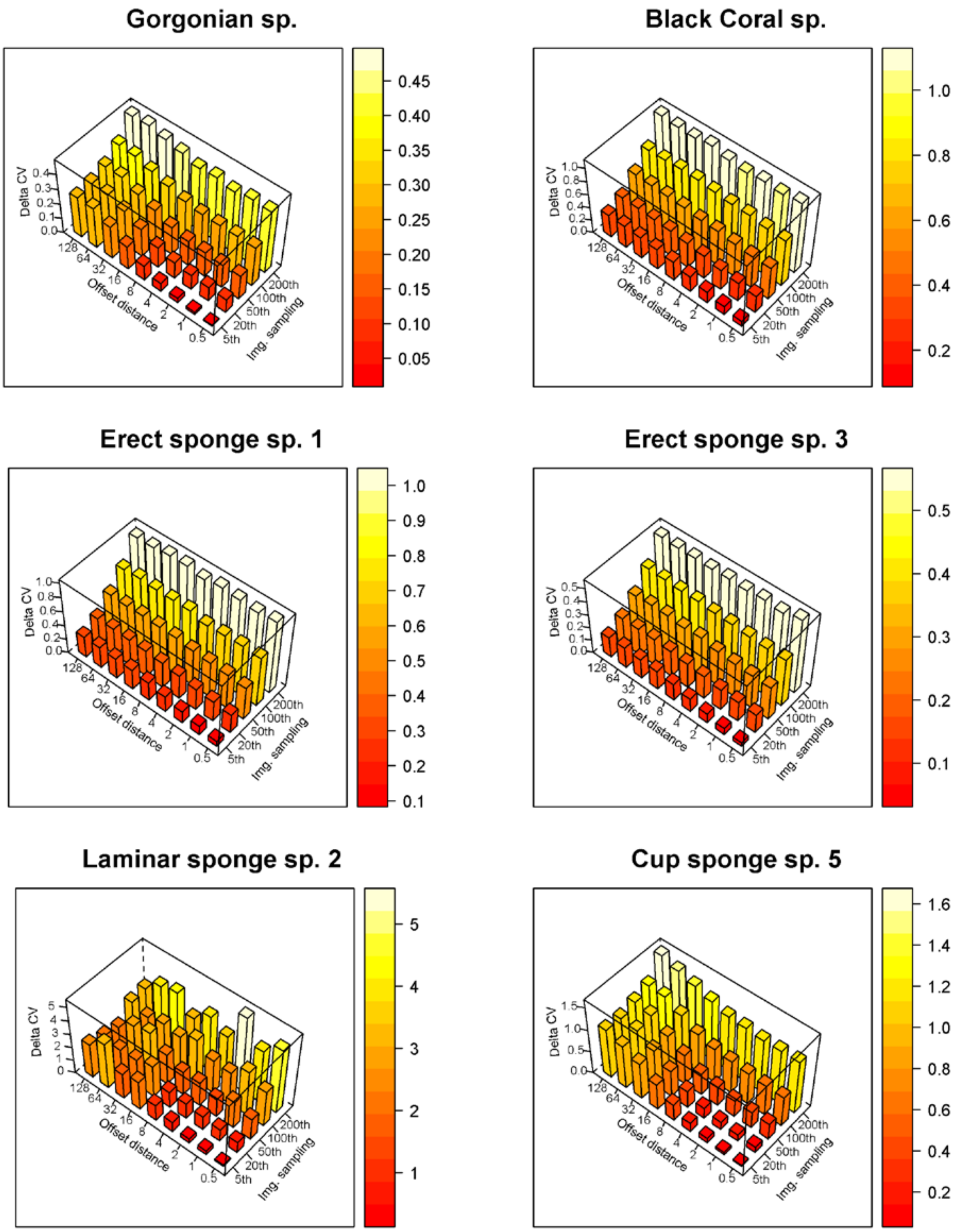
Gorgonian sp.
Black Coral sp.
Erect sponge sp. 1
Erect sponge sp. 3
Laminar sponge sp. 2
Cup sponge sp. 5
Delta CV
Offset distance
Img. sampling
128
64
32
16
8
4
2
1
0.5
5th
20th
50th
100th
200th

Figure 6

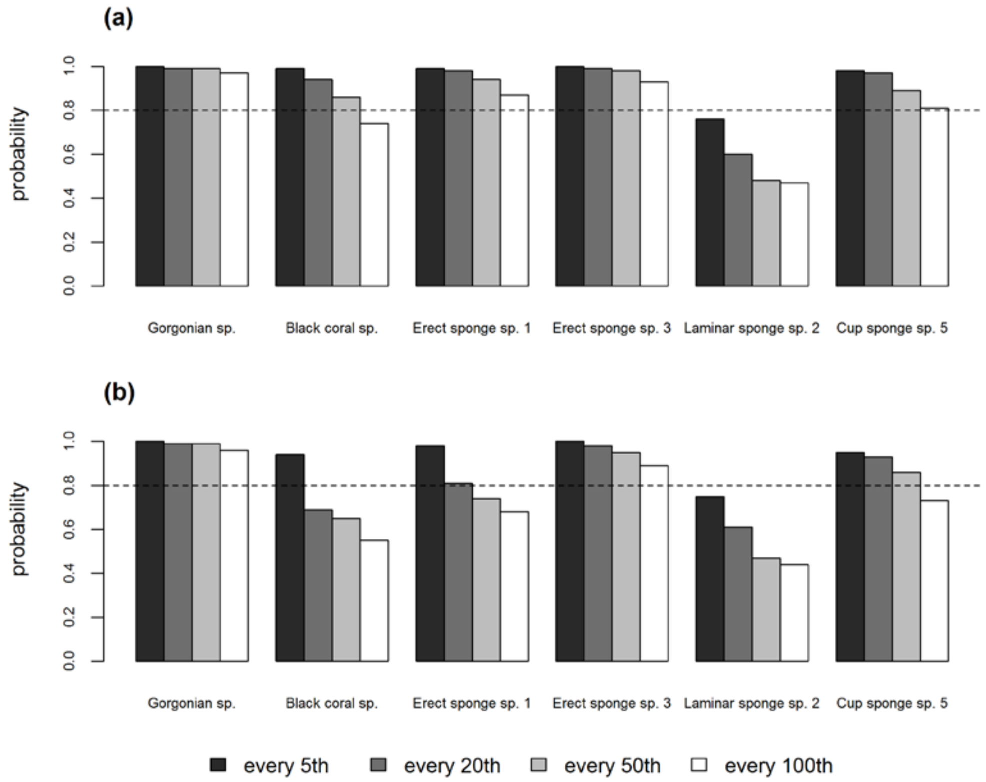
(a)
probability
0.0
0.2
0.4
0.6
0.8
1.0
Gorgonian sp.
Black coral sp.
Erect sponge sp. 1
Erect sponge sp. 3
Laminar sponge sp. 2
Cup sponge sp. 5
(b)
probability
0.0
0.2
0.4
0.6
0.8
1.0
Gorgonian sp.
Black coral sp.
Erect sponge sp. 1
Erect sponge sp. 3
Laminar sponge sp. 2
Cup sponge sp. 5
every 5th
every 20th
every 50th
every 100th